Interface sensitivity in electron/ion yield X-ray absorption spectroscopy: the TiO₂–H₂O interface

Matthijs A. van Spronsen^{1,2,*,†}, Xiao Zhao^{2,3,†}, Maximilian Jaugstetter⁴, Carlos Escudero⁵, Tomáš Duchoň⁶, Adrian Hunt⁷, Iradwikanari Waluyo⁷, Peidong Yang^{2,8}, and Miquel B. Salmeron^{2,3,*}

¹Diamond Light Source Ltd, Didcot, UK

²Materials Sciences Department, Lawrence Berkeley National Laboratory, Berkeley, CA, USA

³Department of Material Science & Engineering, UC Berkeley, Berkeley, CA, USA

⁴Department of Chemistry and Biochemistry, Ruhr-University-Bochum, Bochum, Germany

⁵ALBA Synchrotron Light Source, Barcelona, Spain

⁶Peter Grünberg Institute PGI-6, Forschungszentrum Jülich GmbH, Jülich, Germany

⁷National Synchrotron Light Source II, Brookhaven National Laboratory, Upton, NY, USA

⁸Department of Chemistry, UC Berkeley, Berkeley, CA, USA

AUTHOR INFORMATION

[†]Contributed equally

Corresponding Authors

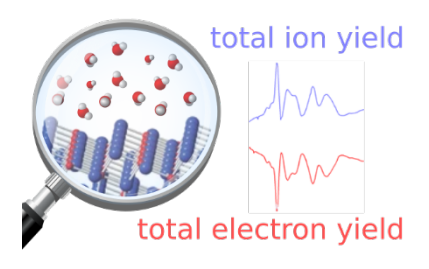
*Matthijs A. van Spronsen (<u>matthijs.vanspronsen@diamond.ac.uk</u>) and Miquel B. Salmeron (<u>mbsalmeron@lbl.gov</u>)

Abstract. To understand corrosion, energy storage, (electro)catalysis, etc., obtaining chemical

information on the solid–liquid interface is crucial but remains extremely challenging. Here, X-ray absorption spectroscopy (XAS) is used to study the solid–liquid interface between TiO₂ and H₂O. A thin film (6.7 nm) of TiO₂ is deposited on an X-ray transparent SiN_x window, acting as the working electrode in a three-electrode flow cell. The spectra are collected based on the electron emission resulting from the decay of the X-ray-induced core-hole-excited atoms, which we show is sensitive to the solid–liquid interface within a few nm. The drain currents measured at the working and counter electrodes are identical but of opposite sign. With this method, we found that the water layer next to anatase is spectroscopically similar to ice. This result highlights the potential of electron-yield XAS to obtain chemical and structural information with a high sensitivity for the species at the electrode–electrolyte interface.

TOC GRAPHICS

TiO₂-H₂O interface



X-ray absorption spectroscopy

KEYWORDS Solid–liquid interface, titanium dioxide (TiO₂), Near-edge X-ray absorption fine structure (NEXAFS), X-ray absorption spectroscopy (XAS), Atomic layer deposition (ALD)

Solid–liquid interfaces are ubiquitous and involved in numerous natural processes and practical applications, such as wetting, corrosion, (electrochemical) catalysis, energy storage, *etc*.

Determining the composition, structure, and chemical state of interfaces, in particular the structure of liquids near electrodes, is crucial to obtain a molecular/atomic understanding of the interfacial processes needed to further improve their applications. Currently, this is hampered by the shortage of appropriate characterization tools.^{1,2} Tools based on electrons are powerful but suffer from impedingly strong attenuation by the liquid phase, whereas those based on photons typically provide mostly information on the bulk phases.

Soft X-ray absorption spectroscopy (XAS) can provide information on both bulk phases of most materials and on their interface with the surrounding environment, *i.e.* vacuum, gas, or liquid. X-ray absorption can be measured directly by attenuation of the primary photons during transmission or indirectly by measuring decay products, fluorescent photons or electrons, produced by the decay of excited core-hole states of the atoms absorbing the X-ray photons. XAS is bulk sensitive when measured in transmission or via fluorescence. Conversely, in the electron yield mode XAS can be highly interface sensitive.

For the solid–vacuum interface only electrons excited near the surface contribute to the measured signal. Soft X-ray absorption leads to the emission of Auger electrons with kinetic energies of hundreds of eV, generating a cascade of secondary electrons as they propagate through the material. Near the interface they can escape into the vacuum. Deeper in the sample the electrons and ions recombine before the electrons reach the surface. The electrons that escape into the vacuum can be measured directly or the so-called drain current is measured, flowing to the sample to neutralize it. Because electron-yield XAS in vacuum gives information on the (near) surface, electron-yield XAS within a liquid cell has also been expected to be sensitive to the solid—liquid interface.^{3,4}

XAS combined with liquid cells enclosed by pressure-resistant, X-ray transparent membranes hold the promise of being an excellent technique to probe solid–liquid interfaces. The first XAS experiments on solid–liquid interfaces with the current measured at the sample (working electrode) were performed on H₂O–Au and H₂SO₄(aq)–Pt interfaces by probing the O K-edge excitation at different bias potentials.^{3,4} Interface sensitivity was assumed from the short inelastic mean free path in water for electrons excited near the interface, hence molecular level understanding of the water–Au adsorption structure and the chemical species near the Pt electrode were derived. In addition to O K-edge spectra, L-edge spectra of Ni and Cu at the interfaces of Ni–NaHCO₃(aq) and Cu–CH₃OH(aq) were reported,⁵ further supporting that electron-yield XAS provides information on the solid–liquid interface.

Recently, an alternative configuration was introduced based on measuring the ionic current at the counter electrode, ^{6,7} connected to the positive end of the ammeter with its negative end connected to the working electrode (the sample). This configuration was thereafter referred to as "total ion yield". Based on the macroscopic travel distances of ions in liquids, it was claimed that the total ion current contains information predominantly from the bulk liquid rather than the interface.⁷ This total ion yield was afterwards used alongside fluorescence yield to probe the L edge of Fe(NO₃)₂(aq),⁶ the C K edge of aqueous dispersions of carbon quantum dots,⁸ and the Mn K edge of aqueous Mn salts.⁹ However, the spectra obtained via total ion yield differed significantly from the truly bulk-sensitive fluorescence yield spectra.

In this letter we show that: (a) the total electron yield and the total ion yield currents are identical but of opposite sign, as expected from charge conservation, and (b) both currents are very sensitive to the interface region extending a few nm into the liquid. The interface sensitivity allows us to reveal a thin ice-like water layer at the interface with anatase TiO₂.

The electrochemical flow cell used in this study (**Figure 1**) was made of PEEK (polyether ether ketone), a highly electrically insulating material, ¹⁰ and sealed by an X-ray-transparent 100-nm-thick SiN_x membrane. Onto this membrane, a layered structure comprising TiO₂/Au/Cr was deposited with respective thicknesses of 6.6/10/2 nm, with TiO₂ facing the water inside the cell. The TiO₂ was deposited using plasma-enhanced atomic layer deposition after Au and Cr were deposited using thermal evaporation. Infrared spectroscopy (Section S2, supporting information) revealed that the structure of the TiO₂ is that of the anatase phase.

The cell was loaded in the end station of the IOS beamline at the National Synchrotron Light Source-II, at the Brookhaven National Laboratory, 11 and at beamline 8.0.1 at the Advanced Light Source, at the Lawrence Berkeley National Laboratory. Deionized H_2O (Milli-Q 18.2 $M\Omega$) was used without further degassing. As a reference, the X-ray absorption spectra for the same $TiO_2/Au/Cr$ stack on SiN_x were also measured under ultrahigh vacuum (UHV), using total electron yield.

Drain currents in this study were measured at the counter electrode with the working electrode grounded (**Figure 1**a), or at the working electrode with the counter electrode grounded (**Figure 1**b). The choice of electrode where the current is measured determines the name used: "total ion yield" if measured at the counter electrode (**Figure 1**a)⁶⁻⁹ and "total electron yield" if measured at the sample/working electrode (**Figure 1**b).³⁻⁵ To avoid confusion, here we refer to them as counter-electrode drain current (**Figure 1**a) and working-electrode drain current (**Figure 1**b). Note that the total electron yield as depicted in **Figure 1**b is different from the "one-electrode" total electron yield described in Ref., ¹² in which, by keeping the counter electrode floating, no signal from inside the cell could be measured.

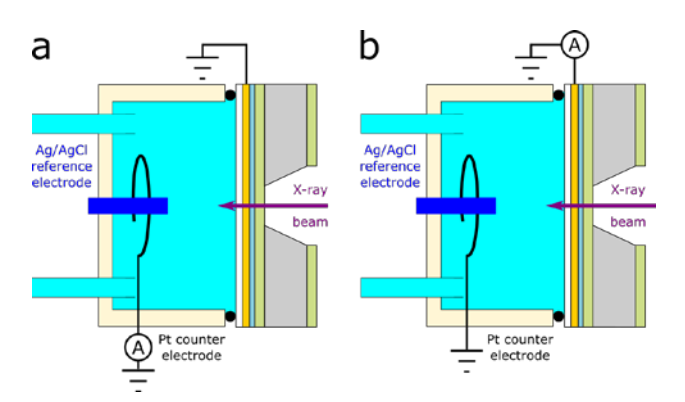


Figure 1. Electrochemical flow cell, filled with pure H_2O , showing the sample (working electrode) comprising three layers: TiO_2 (6.6 nm, white) facing the electrolyte, Au (10 nm, yellow), and Cr (2 nm, blue) on a free-standing, X-ray-transparent SiN_x film (100 nm×1 mm², green), supported on a Si frame (gray). Drain currents are measured at the counter electrode (a) or at the working electrode (b), each with the other electrode grounded.

Comparison of the counter-electrode and working-electrode drain currents shows that they are inverted relative to each other but otherwise practically identical (**Figure 2**a). This is emphasized by the near complete overlap between the inverted working-electrode drain current and the counter-electrode drain current (**Figure 2**b), clearly showing that both signals contain the same information.

Spectroscopically, the Ti L-edge spectra (**Figure 2**) contain all the features typically observed for TiO₂, which are ascribed to Ti $2p\rightarrow 3d$ transitions. The L edge is split into two components because of spin-orbit coupling. These two are labeled L₃ and L₂ and related to excitation from Ti $2p_{3/2}$ and $2p_{1/2}$, respectively. Both components are further divided into two peaks, originating in the crystal-field splitting of the Ti 3d band and assigned to Ti $2p\rightarrow t_{2g}$ and $2p\rightarrow e_g$. Finally, the L₃-e_g peak comprises two closely spaced maxima with their relative intensity depending on, among other things, the TiO₂ crystal structure. The origin for the L₃-e_g splitting is debated: short-scale distortions in the bonding in the TiO₆, Ta, Tange distortions

between octahedrons, 15,16 and dynamic coupling of electronic and vibrational states 17,18 have been proposed.

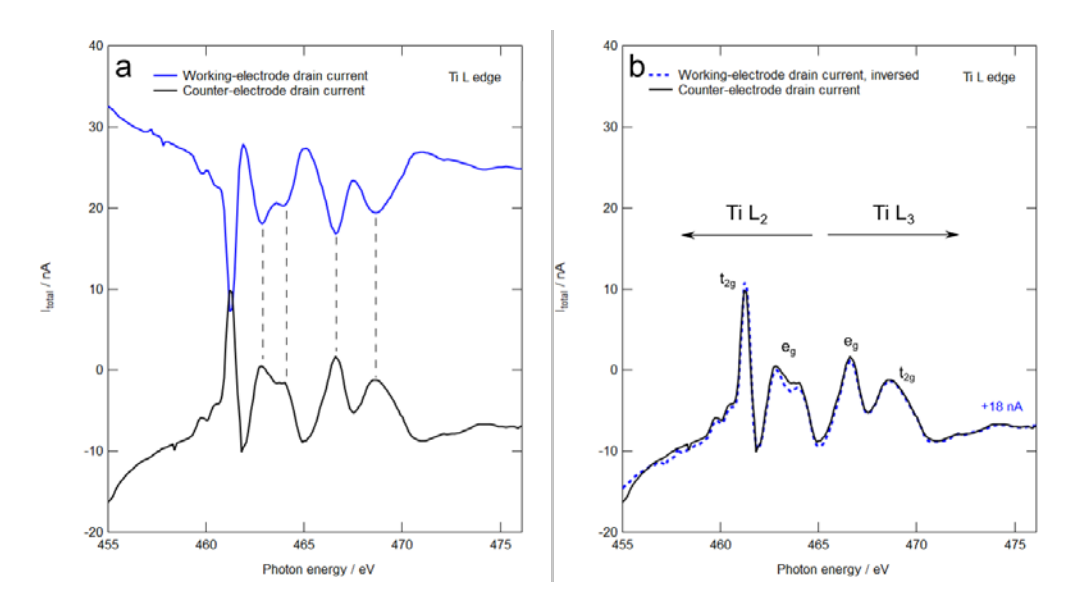


Figure 2. Ti L-edge spectra of TiO₂ in deionized water (a), measured via the counter-electrode (black) or via the working-electrode drain current (blue). Similarities are highlighted by inverting and overlaying the working-electrode drain current (b).

Both the counter and working-electrode drain currents originate in X-ray absorption at the working electrode–liquid interface because Ti is only present in the 6.6-nm-thick TiO₂ film in the working electrode. The TiO₂ film was stable for hours in the liquid under irradiation by the X-ray beam, indicating negligible leaching of Ti and/or redeposition on the counter electrode (a Pt wire). Furthermore, the soft X-rays are fully absorbed by the liquid and cannot reach the counter electrode (transmission of X-rays up to 1 keV through 0.15 mm H₂O is less than a ppm,¹⁹ and the typical electrode separation is several millimeters).

It may seem counter-intuitive that the spectrum of the H₂O-TiO₂ interface can be measured via the counter-electrode drain current, given the short inelastic mean free path of electrons in liquids, around 1–2 nanometers.²⁰ The mechanism of the charge transfer from working to counter electrode is not yet clearly understood. However, a crucial step is the emission of energetic Auger and secondary electrons from the working electrode into the liquid, ionizing the liquid, and leading to a multitude of positive ions and secondary electrons. As the electrons lose energy, they may recombine with cations, get attached to neutral molecules creating anions, or become solvated electrons. In this thermalization process, a cascade of charged species is generated, possibly with longer lifetimes and diffusion lengths. The transport pathway of these species is interesting and deserves careful investigation, likely needing additional experiments. This is, however, outside of the goals of this work.

The observation that both drain currents carry the same signal is not unexpected because the cell walls are electrically insulated. To maintain charge neutrality, all electrons flowing into the liquid cell via one electrode must be balanced by the same number of electrons leaving the cell via the other electrode. The spectra are inverted because they represent the same current measured in opposite directions. In **Figure 2**, the current was such that electrons entered the cell via the counter electrode and left via the working electrode. Even though X-ray absorption initially leads to the emission of Auger (and secondary) electrons from the working electrode into the liquid, more secondary electrons generated in the liquid leave the cell via the working electrode. Because both drain currents are essentially the same signal, distinction between "total ion yield and "total electron yield" is not very meaningful. It is also confusing because total ion yield XAS is employed in liquid-jet experiments or in ionization chambers, where the primary ionized atom can actually be measured. The solid-liquid XAS measurements resemble more

the conversion electron yield detection, which has been established for XAS on the solid-gas interface.²³

Focusing on the O K-edge spectrum of the TiO₂–H₂O system (**Figure 3**a), the spectral features of TiO₂ can be clearly recognized between 530 and 535 eV, partially overlapping with features from the oxygen of H₂O above approximately 535 eV. Comparing the TiO₂–H₂O spectrum with that obtained from TiO₂ alone, *i.e.* in UHV (**Figure 3**b), shows the H₂O contribution to the TiO₂–H₂O spectrum is modest, further confirming the surface sensitivity of the spectra collected via the counter-electrode drain current.

Both the spectra for TiO₂–H₂O and TiO₂–UHV have two sharp peaks assigned to O 1s \rightarrow t_{2g} and O 1s \rightarrow e_g transitions in TiO₂. These transitions are dipole-allowed through the hybridization of the O 2p and Ti 3d orbitals. The broad features above 535 are assigned to transitions to higher unoccupied orbitals, O 1s \rightarrow a_{1g} and O 1s \rightarrow t_{1u}. Some differences between the TiO₂–H₂O and TiO₂–UHV spectra are visible, such as a weak shoulder around 535 eV, an increase in edge intensity starting at 537 eV, and a broad peak around 542.7eV.

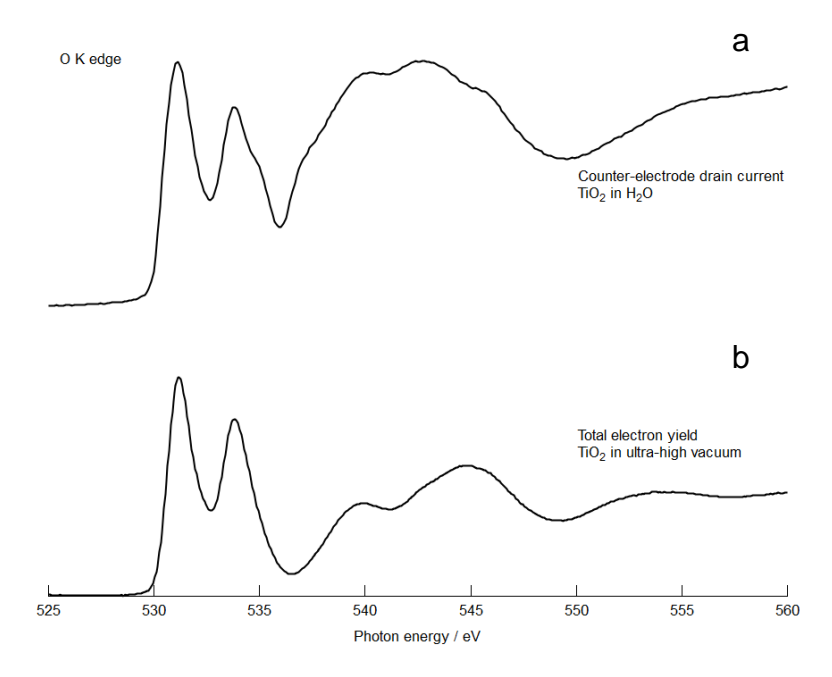


Figure 3. O K-edge spectra of (a) TiO₂ in deionized water measured via the counter-electrode drain current (**Figure 1**a) and of (b) TiO₂ under UHV measured via the conventional total electron yield.

Subtraction of the TiO₂–UHV spectrum from that of TiO₂–H₂O unveils the spectral contribution of H₂O (black curve, **Figure 4**). The difference spectrum shows a remarkable similarity with that of ice at 268 K (red curve, **Figure 4**). At this temperature, the surface of the ice is premelted and covered by a *ca.* 1-nm-thick layer of liquid water.²⁶ Interestingly, *ab initio* molecular dynamics by Selloni et al. predict that water on anatase TiO₂ forms a stable bilayer of molecules with ice-like dynamics.¹⁸ In addition to the ice similarity, close inspection of the difference spectrum reveals additional features between 529.5 and 533 eV, which cannot be attributed to H₂O, hinting at other unique features of the TiO₂–H₂O interface.

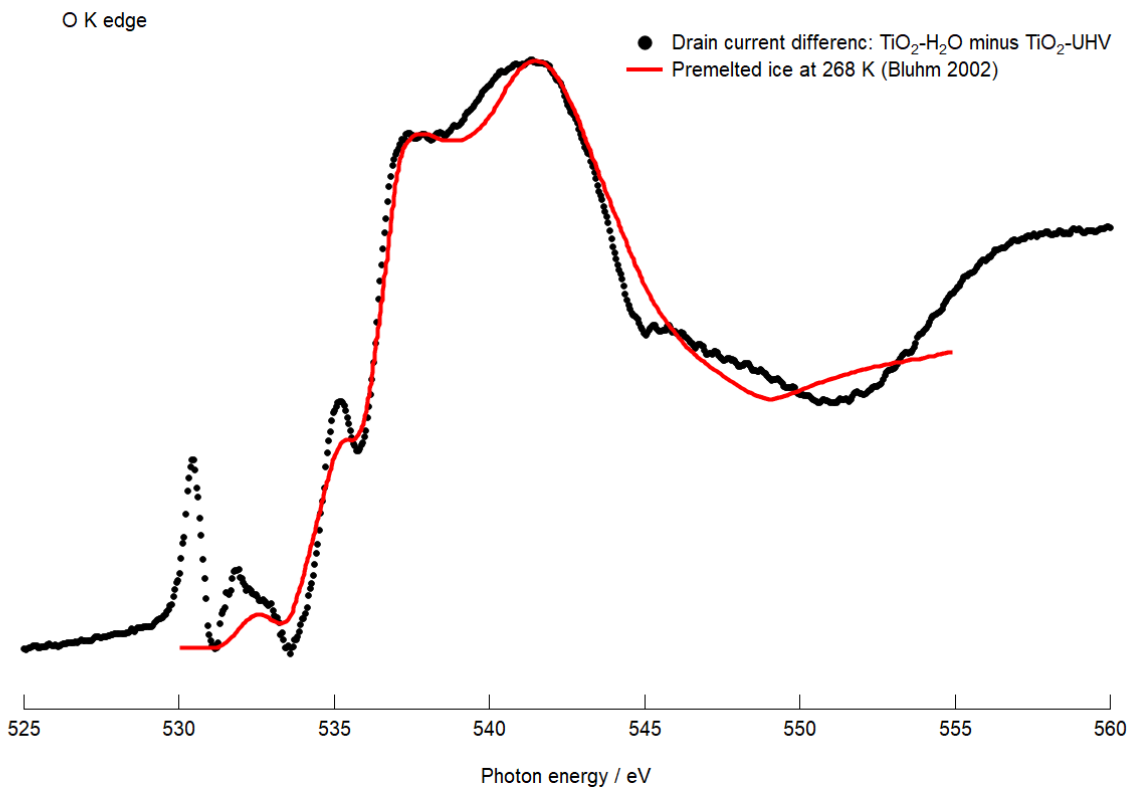


Figure 4. Difference spectrum (black) obtained by subtracting the O K edge spectrum of TiO_2 in UHV (**Figure 3**b) from that of TiO_2 in H_2O (**Figure 3**a), after scaling to match the O $1s \rightarrow t_{2g}$ peak intensity (531.1 eV). The difference spectrum has been corrected for X-ray absorption by the SiN_x . The difference spectrum closely resembles the spectrum (red) of ice during the melting transition (reproduced with permission from Ref. ²⁶ using webPlotDigitizer²⁷).

Comparing the relative contributions of TiO₂ and H₂O shows that TiO₂ is the major contributor to the O K-edge spectrum of TiO₂–H₂O. Assuming that the intensity in the difference spectrum above 533.4 eV stems from H₂O, yields a TiO₂: H₂O contribution ratio of 1.4. Since the TiO₂ thickness (6.6 nm) is accurately known based on the self-limiting growth characteristic of atomic-layer deposition, this puts an upper limit on the probed H₂O(l) region of *ca.* 10 nm extending from the TiO₂–H₂O interface, considering the 2.4-times higher atomic density of O in TiO₂ compared to H₂O(l). This estimation is supported by molecular dynamics simulations,²⁸

which predicted that the thickness of the ice-like interfacial water is 2 layers. The clear contribution of this thin interfacial water to the spectrum suggests that only a few liquid layers

are probed beyond the interfacial region, thus putting the interface sensitivity closer to 1–2 nm.

A precise determination of the probed H₂O(1) layer is complex and is likely to depend on

the relative amplification of the signal by the generation of secondary electrons in the solid and

liquid phases. Additionally, the separation of the O K-edge signal contributions from H₂O and

TiO₂ will influence the analysis.

In summary, our XAS work on the solid-liquid interface shows that the recently

introduced^{6,7} total ion yield is essentially the same as the total electron yield reported earlier,^{3,4,29}

and both are highly surface sensitive. This encouraging result shows that drain-current XAS is a

promising tool to study interface phenomena and provides the first experimental confirmation of

the presence of ice-like interfacial water near TiO₂, predicted to be only two layers thick.

ASSOCIATED CONTENT

Supporting Information.

The following file is available free of charge.

Details regarding sample preparation, characterization, and beamline measurements (PDF)

AUTHOR INFORMATION

Notes

The authors declare no competing financial interests.

ACKNOWLEDGMENT

12

This research was supported by the U.S. Department of Energy, Office of Science, Basic Energy Sciences, Materials Sciences and Engineering Division, under Contract No. DE-AC02-05-CH11231 within the Structure and Dynamics of Materials Interfaces program KC31SM. This research used beamline 23-ID-2 (IOS) of the National Synchrotron Light Source II, a U.S. Department of Energy (DOE) Office of Science User Facility operated for the DOE Office of Science by Brookhaven National Laboratory under Contract No. DE-SC0012704. This research used beamline 8.0.1 of the Advanced Light Source, a U.S. DOE Office of Science User Facility under contract no. DE-AC02-05CH11231. Support by Yi-Sheng Liu, Feipeng Yang, and Jinghua Guo of ALS beamline 8.0.1 is gratefully acknowledged. Sample preparation and FTIR measurements at the Molecular Foundry were supported by the Office of Science, Office of Basic Energy Sciences, of the U.S. Department of Energy under Contract No. DE-AC02-05CH11231. X.Z was supported by an NSF-BSF grant number 1906014.

REFERENCES

- Zaera, F. Surface Chemistry at the Liquid/Solid Interface. Surf. Sci. 2011, 605 (13–14),
 1141–1145. https://doi.org/10.1016/j.susc.2011.04.021.
- (2) Timoshenko, J.; Roldan Cuenya, B. In Situ/ Operando Electrocatalyst Characterization by X-Ray Absorption Spectroscopy. *Chem. Rev.* 2021, 121 (2), 882–961. https://doi.org/10.1021/acs.chemrev.0c00396.
- (3) Velasco-Velez, J. J.; Wu, C. H.; Pascal, T. A.; Wan, L. F.; Guo, J.; Prendergast, D.; Salmeron, M. The Structure of Interfacial Water on Gold Electrodes Studied by X-Ray Absorption Spectroscopy. *Science* 2014, 346 (6211), 831–834. https://doi.org/10.1126/science.1259437.
- (4) Wu, C. H.; Pascal, T. A.; Baskin, A.; Wang, H.; Fang, H.-T.; Liu, Y.-S.; Lu, Y.-H.; Guo,

- J.; Prendergast, D.; Salmeron, M. B. Molecular-Scale Structure of Electrode–Electrolyte Interfaces: The Case of Platinum in Aqueous Sulfuric Acid. *J. Am. Chem. Soc.* **2018**, *140* (47), 16237–16244. https://doi.org/10.1021/jacs.8b09743.
- Weatherup, R. S.; Wu, C. H.; Escudero, C.; Pérez-Dieste, V.; Salmeron, M. B. (5) Radiation Damage Environment-Dependent in Atmospheric Pressure X-Ray Spectroscopy. J. Phys. Chem. В 2018, 122 (2),737-744. https://doi.org/10.1021/acs.jpcb.7b06397.
- (6) Schön, D.; Xiao, J.; Golnak, R.; Tesch, M. F.; Winter, B.; Velasco-Velez, J. J.; Aziz, E. F. Introducing Ionic-Current Detection for X-Ray Absorption Spectroscopy in Liquid Cells. J. Phys. Chem. Lett. 2017, 8 (9), 2087–2092. https://doi.org/10.1021/acs.jpclett.7b00646.
- (7) Schön, D.; Golnak, R.; Tesch, M. F.; Winter, B.; Velasco-Velez, J. J.; Aziz, E. F.; Xiao, J. Bulk-Sensitive Detection of the Total Ion Yield for X-Ray Absorption Spectroscopy in Liquid Cells. J. Phys. Chem. Lett. 2017, 8 (20), 5136–5140. https://doi.org/10.1021/acs.jpclett.7b02381.
- (8) Ren, J.; Achilleos, D. S.; Golnak, R.; Yuzawa, H.; Xiao, J.; Nagasaka, M.; Reisner, E.; Petit, T. Uncovering the Charge Transfer between Carbon Dots and Water by in Situ Soft X-Ray Absorption Spectroscopy. *J. Phys. Chem. Lett.* 2019, 10 (14), 3843–3848. https://doi.org/10.1021/acs.jpclett.9b01800.
- (9) Xi, L.; Schellenberger, M.; Präg, R. F.; Golnak, R.; Schuck, G.; Lange, K. M. Ionic Current Mn K-Edge X-Ray Absorption Spectra Obtained in a Flow Cell. J. Phys. Chem. C 2018, 122 (27), 15588–15594. https://doi.org/10.1021/acs.jpcc.8b04693.
- (10) Das-Gupta, D. K.; Doughty, K. Dielectric and Conduction Processes in Polyetherether Ketone (PEEK). *IEEE Trans. Electr. Insul.* **1987**, *EI-22* (1), 1–7.

- https://doi.org/10.1109/TEI.1987.298955.
- (11) Palomino, R. M.; Stavitski, E.; Waluyo, I.; Chen-Wiegart, Y. K.; Abeykoon, M.; Sadowski, J. T.; Rodriguez, J. A.; Frenkel, A. I.; Senanayake, S. D. New In-Situ and Operando Facilities for Catalysis Science at NSLS-II: The Deployment of Real-Time, Chemical, and Structure-Sensitive X-Ray Probes. *Synchrotron Radiat. News* 2017, 30 (2), 30–37. https://doi.org/10.1080/08940886.2017.1289805.
- (12) Schön, D.; Xiao, J.; Golnak, R.; Tesch, M. F.; Winter, B.; Velasco-Velez, J. J.; Aziz, E. F. Introducing Ionic-Current Detection for X-Ray Absorption Spectroscopy in Liquid Cells. *Journal of Physical Chemistry Letters*. 2017, pp 2087–2092. https://doi.org/10.1021/acs.jpclett.7b00646.
- (13) de Groot, F. M. F.; Figueiredo, M. O.; Basto, M. J.; Abbate, M.; Petersen, H.; Fuggle, J. C. 2 p X-Ray Absorption of Titanium in Minerals. *Phys. Chem. Miner.* 1992, 19 (3), 140–147. https://doi.org/10.1007/BF00202101.
- (14) Ruus, R.; Kikas, A.; Saar, A.; Ausmeesb E Ndmmiste, O. A.; Aarik, J.; Aidla, A.; Uustared, T. *Ti 2p AND 0 1s X-RAY ABSORPTION OF TiOz POLYMORPHS*; 1997; Vol. 104.
- (15) Crocombette, J. P.; Jollet, F. Ti 2p X-Ray Absorption in Titanium Dioxides (TiO2): The Influence of the Cation Site Environment. *J. Phys. Condens. Matter* **1994**, *6* (49), 10811–10821. https://doi.org/10.1088/0953-8984/6/49/022.
- (16) Krüger, P. Multichannel Multiple Scattering Calculation of L2,3 -Edge Spectra of TiO2 and SrTiO3: Importance of Multiplet Coupling and Band Structure. *Phys. Rev. B Condens. Matter Mater. Phys.* 2010, 81 (12), 125121. https://doi.org/10.1103/PhysRevB.81.125121.

- (17) Brydson, R.; Sauer, H.; Engel, W.; Thomass, J. M.; Zeitler, E.; Kosugi, N.; Kuroda, H. Electron Energy Loss and X-Ray Absorption Spectroscopy of Rutile and Anatase: A Test of Structural Sensitivity. *J. Phys. Condens. Matter* **1989**, *1* (4), 797–812. https://doi.org/10.1088/0953-8984/1/4/012.
- (18) Fronzoni, G.; De Francesco, R.; Stener, M.; Causà, M. X-Ray Absorption Spectroscopy of Titanium Oxide by Time Dependent Density Functional Calculations. *J. Phys. Chem. B* 2006, 110 (20), 9899–9907. https://doi.org/10.1021/jp057353a.
- (19) Henke, B. L.; Gullikson, E. M.; Davis, J. C. X-Ray Interactions: Photoabsorption, Scattering, Transmission, and Reflection at E=50-30000 EV, Z=1-92. *At. Data Nucl. Data Tables* **1993**, *54*, 181–342.
- (20) Shinotsuka, H.; Da, B.; Tanuma, S.; Yoshikawa, H.; Powell, C. J.; Penn, D. R. Calculations of Electron Inelastic Mean Free Paths. XI. Data for Liquid Water for Energies from 50 EV to 30 KeV. Surf. Interface Anal. 2017, 49 (4), 238–252. https://doi.org/10.1002/sia.6123.
- (21) Wilson, K. R.; Tobin, J. G.; Ankudinov, A. L.; Rehr, J. J.; Saykally, R. J. Extended X-Ray Absorption Fine Structure from Hydrogen Atoms in Water. *Phys. Rev. Lett.* **2000**, *85* (20), 4289–4292. https://doi.org/10.1103/PhysRevLett.85.4289.
- Wilson, K. R.; Rude, B. S.; Catalane, T.; Schaller, R. D.; Tobin, J. G.; Co, D. T.; Saykally,
 R. J. X-Ray Spectroscopy of Liquid Water Microjets. *J. Phys. Chem. B* 2001, 105 (17),
 3346–3349. https://doi.org/10.1021/jp010132u.
- (23) Tamenori, Y. Synchrotron Radiation Electron Yield Soft X-Ray Photoabsorption Spectroscopy under Normal Ambient-Pressure Conditions. *J. Synchrotron Rad* **2013**, *20*, 419–425. https://doi.org/10.1107/S0909049513003592.

- (24) Fischer, D. W. X-Ray Band Spectra and Molecular-Orbital Structure of Rutile TiO2. *Phys. Rev. B* **1972**, *5* (11), 4219–4226. https://doi.org/10.1103/PhysRevB.5.4219.
- (25) Grunes, L. A.; Leapman, R. D.; Wilker, C. N.; Hoffmann, R.; Kunz, A. B. Oxygen K Near-Edge Fine Structure: An Electron-Energy-Loss Investigation with Comparisons to New Theory for Selected 3d Transition-Metal Oxides. *Phys. Rev. B* 1982, 25 (12), 7157–7173. https://doi.org/10.1103/PhysRevB.25.7157.
- (26) Bluhm, H.; Ogletree, D. F.; Fadley, C. S.; Hussain, Z.; Salmeron, M. The Premelting of Ice Studied with Photoelectron Spectroscopy. *J. Phys. Condens. Matter* **2002**, *14* (8), 227–233. https://doi.org/10.1088/0953-8984/14/8/108.
- (27) Rohatgi, A. WebPlotDigitizer. Pacifica, CA, USA 2020.
- (28) Calegari Andrade, M. F.; Ko, H. Y.; Car, R.; Selloni, A. Structure, Polarization, and Sum Frequency Generation Spectrum of Interfacial Water on Anatase TiO 2. *J. Phys. Chem. Lett.* **2018**, *9* (23), 6716–6721. https://doi.org/10.1021/acs.jpclett.8b03103.
- (29)Weatherup, R. S.; Wu, C. H.; Escudero, C.; Pérez-Dieste, V.; Salmeron, M. B. Environment-Dependent Radiation Damage Atmospheric in Pressure X-Ray В Spectroscopy. J. Phys. Chem. 2018. 122 (2),737–744. https://doi.org/10.1021/acs.jpcb.7b06397.